Spectroscopic Characterization of the Atomic Hydrogen Energies and Densities and Carbon Species during Helium−Hydrogen−Methane Plasma CVD Synthesis of Diamond Films

Randell Mills,* Jayasree Sankar, Paresh Ray, Bala Dhandapani, and Jiliang He

BlackLight Power, Inc., 493 Old Trenton Road, Cranbury, New Jersey 08512

Received August 6, 2002. Revised Manuscript Received November 25, 2002

Polycrystalline diamond films were synthesized on silicon substrates for the first time without diamond seeding by a very low power (38 W) microwave plasma chemical vapor deposition reaction of a mixture of helium−hydrogen−methane (48.2/48.2/3.6%). The films were characterized by time-of-flight secondary ion mass spectroscopy, X-ray photoelectron spectroscopy, Raman spectroscopy, scanning electron microscopy, and X-ray diffraction. It is proposed that He^+ served as a catalyst with atomic hydrogen to form an energetic plasma. CH, C_2, and C_3 emissions were observed with significantly broadened H α, β, γ, and δ lines. The average hydrogen atom temperature of a helium−hydrogen−methane plasma was measured to be 120−140 eV versus ≈3 eV for pure hydrogen. Bombardment of the carbon surface by highly energetic hydrogen formed by the catalysis reaction may play a role in the formation of diamond. Then, by this novel pathway, the relevance of the CO tie line is eliminated along with other stringent conditions and complicated and inefficient techniques which limit broad application of the versatility and superiority of diamond thin film technology.

I. Introduction

Diamond has some of the most extreme physical properties of any material such as outstanding mechanical strength, optical transparency, high thermal conductivity, high electron mobility, and unique chemical properties.[1] Thus, a variety of possible applications are envisioned for diamond materials. Yet its practical use in applications has been limited due to its scarcity, expense, and immalleability. The development of techniques for depositing thin films of synthetic diamonds on a variety of substrates has enabled the exploitation of diamond's superlative properties in many new and exciting applications. These include cutting tools, thermal management of integrated circuits, optical windows, high-temperature electronics, surface acoustic wave (SAW) filters, field emission displays, electrochemical sensors, composite reinforcement, microchemical devices and sensors, and particle detectors.[1] But the fundamental impediment facing the technology at the present is insufficient growth rate of high-quality diamond under milder conditions.

Synthetic diamond was initially commercially produced as single crystals using the so-called high-pressure high-temperature (HPHT) growth technique[1] wherein graphite is compressed in a hydraulic press to tens of thousands of atmospheres, heated to over 2000 K, and left until diamond crystallizes. Recent novel HPHT methods which have been largely unsuccessful, except for the production of nanocrystals by Orwa et al.,[2] are based on attempts to use high-energy ion implantation to bury carbon deep in metals or fused silica to take advantage of the large confining pressures there. More versatile thin films have been produced by an addition-of-one-atom-at-a-time approach using chemical vapor deposition (CVD) techniques. All CVD techniques for producing diamond films require activation of the gaseous carbon-containing precursor molecules. To promote diamond over graphite growth, the precursor gas is usually CH_4, which is diluted in excess hydrogen that is typically 99% of the reactant mixture, and the temperature of the substrate is usually maintained in excess of 700 °C. Activation may be achieved thermally using a hot filament, gas discharge such as dc, rf, or microwave discharges, or a combustion flame such as an oxyacetylene torch.[1]

Although the mechanism of diamond growth on a seed of diamond is still not well understood, it is believed to be based on the extraction of H of a CH terminal bond to form a dangling carbon center to which CH_3 reacts. A carbon−carbon bond forms between adjacent methyl groups, and the hydrogen is gradually extracted, probably by H forming H_2. Further preferential etching of graphitic carbon over diamond carbon by hydrogen permits diamond growth.[1] H may also be required to decrease the concentration of gas-phase unsaturated hydrocarbons.

More recent advances of diamond formation have been toward developing methods to grow diamond at low temperatures (<500 °C rather than 700 °C) such

* Corresponding author. Phone: 609-490-1090. Fax: 609-490-1066. E-mail: rmills@blacklightpower.com.

(1) May, P. W. *Philos. Trans. R. Soc. London A* **2000**, *358*, 473.

(2) Orwa, J. O.; Prawer, S.; Jamieson, D. N.; Peng, J. L.; McCallum, J. C.; Nugent, K. W.; Li, Y. J.; Bursill, L. A. *J. Appl. Phys.* **2001**, *90*, 3007.

10.1021/cm020817m CCC: $25.00
Published on Web 02/20/2003

that diamond films can be grown on a wider range of substrate materials of commercial importance with low melting points such as plastics, aluminum, some glasses, nickel, steel, and electronic materials such as GaAs. Many gas mixtures have been investigated to achieve this goal including ones containing some halogens, presumably substituting for the role played by H.[3] More common mixtures have different combinations of H_2, CH_4, O_2, CO_2, and CO.[3] Quite successful diamond film growth has been achieved at temperatures as low as 180 °C using gas mixtures of CH_4 mixed with CO_2 or CO in microwave plasma deposition reactors wherein an optimal rate is obtained when the gas ratio is about 50/50%. Although the concentration of H_2 in the activated gas mixture is approximately half that seen in the CH_4-H_2 mixtures,[4] the CO_2-CH_4, and $CO-CH_4$ systems are unique in that hydrogen is low compared to the excess needed in other systems, presumably because oxygen species such as O_2, O, and OH in the CO_2-CH_4 and $CO-CH_4$-system plasmas perform the same role as H in the CH_4-H_2-system plasmas. Recent molecular beam mass spectroscopy investigations of the CO_2-CH_4 system indicate the incorporation of CH_3 at a dangling carbon bond is the most probable mechanism as in the case of the CH_4-H_2 system. However, the species that extracts H may not be an oxygen species. Rather, CO may activate the surface by extracting a terminating H.[5]

Empirically, it is known that only a narrow set of ratios of O, C, and H results in diamond formation. Using the combined data from over 70 diamond deposition experiments, Bachmann et al. produced a C−H−O phase diagram for diamond deposition, which showed that low-pressure diamond synthesis is only possible within a very narrow well-defined domain centered on a line called the CO tie line.[6,7] A consequence of this analysis was that the exact nature of the plasma gases was unimportant for most CVD processes; rather, the relative ratios of O, C, and H controlled the deposition.

It was previously reported that a novel highly stable surface coating SiH, which comprised high binding energy hydride ions, was synthesized by microwave plasma reaction of a mixture of silane, hydrogen, and helium, wherein it was proposed that He^+ served as a catalyst with atomic hydrogen to form the highly stable hydride ions.[8] The novel silicon hydride was identified by time-of-flight secondary ion mass spectroscopy (ToF-SIMS) and X-ray photoelectron spectroscopy (XPS). ToF-SIMS identified the coatings as hydride by the large SiH^+ peak in the positive spectrum and the dominant H^- in the negative spectrum. XPS identified the H content of the SiH coatings as hydride ions corresponding to peaks at 11, 43, and 55 eV with no corresponding primary element peaks. The silicon hydride surface was remarkably stable in air for long duration of exposure as shown by XPS.

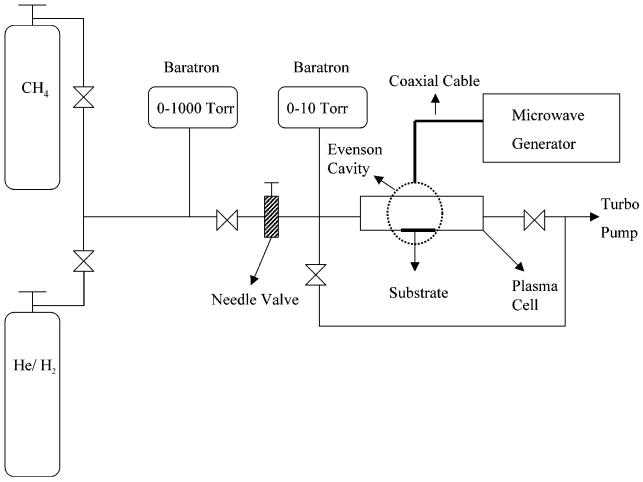

Figure 1. Experimental setup comprising a microwave discharge cell operated under flow conditions.

In the quest for low-temperature diamond synthesis, CH_4 was substituted for SiH_4 in the helium−hydrogen microwave reaction, which formed novel SiH. In this paper, we report the deposition of polycrystalline diamond films on silicon wafers by a helium−hydrogen−CH_4 (48.2/48.2/3.6%) microwave plasma maintained with an Evenson cavity without diamond seeding or abrasion, which provides seed crystals[9] under very mild conditions. After the plasma-processing reaction, the surface was characterized by ToF-SIMS, XPS, Raman spectroscopy, SEM, and X-ray diffraction (XRD). To understand the role of the helium−hydrogen plasma, it was characterized by recording the line broadening of the 656.3-nm Balmer α line to determine the excited hydrogen atom energy.

II. Experimental Section

Synthesis. Diamond films were grown on silicon wafer substrates by their exposure to a low-pressure $He-H_2-CH_4$ microwave plasma. The experimental setup comprising a microwave discharge cell operated under flow conditions is shown in Figure 1. A silicon wafer substrate ($0.5 \times 0.5 \times 0.05$ cm, Silicon Quest International, silicon(100), boron-doped) cleaned by heating to 700 °C under vacuum was placed about 2 cm off center inside of a quartz tube (1.2-cm diameter and 25-cm long) with vacuum valves at both ends. The tube was center-fitted with an Opthos coaxial microwave cavity (Evenson cavity) and connected to the gas/vacuum line. The quartz tube and vacuum line were evacuated for 2 h to remove any trace moisture or oxygen and residual gases. Premixed $He-H_2$ (50/50%) was further mixed with CH_4 such that a $He-H_2-CH_4$ (48.2/48.2/3.6%) gas mixture was introduced through the quartz tube reactor at a total pressure of 3 Torr as monitored by an absolute pressure gauge. The corresponding gas flow rates controlled by mass flow controllers were maintained at 60 and 2.25 sccm for $He-H_2$ and CH_4, respectively. In separate experiments, the helium−hydrogen premixed gas was varied from 90/10% to 50/50%. Since the best diamond film results were obtained with the 50/50% mixture, only these results will be presented.

The microwave generator shown in Figure 1 was an Opthos model MPG-4M generator (frequency: 2450 MHz). The microwave plasma was maintained with a 40 W (forward)/2 W

(3) Elliott, M. A.; May, P. W.; Petherbridge, J.; Leeds, S. M.; Ashfold, M. N. R.; Wang, W. N. *Diamond Relat. Mater.* **2000**, *9*, 311.
(4) Petherbridge, J. R.; May, P. W.; Pearce, S. R. J.; Rosser, K. N.; Ashfold, M. N. R. *J. Appl. Phys.* **2001**, *89*, 1484.
(5) Petherbridge, J.; May, P. W.; Pearce, S. R. J.; Rosser, K. N.; Ashfold, M. N. R. *Diamond Relat. Mater.* **2001**, *10*, 393.
(6) Bachmann, P. K.; Leers, D.; Lydtin, H.; Wiechert, D. U.; *Diamond Relat. Mater.* **1991**, *1*, 1.
(7) Bachmann, P. K.; Hagemann, H. G.; Lade, H.; Leers, D.; Picht, F.; Wiechert, D. U. *Mater. Res. Soc. Proc.* **1994**, *339*, 267.
(8) Mills, R. L.; He, J.; P. Ray, Dhandapani, B.; Chen, X. *Int. J. Hydrogen Energy*, in press.
(9) Rebello, J. H. D.; Straub, D. L.; Subramaniam, V. V. *J. Appl. Phys.* **1992**, *72*, 1133.

(reflected) power for about 12−16 h. The substrate was at the cool edge of the plasma glow region. The wall temperature at this position measured with a contacting thermocouple was about 300 °C. A thick (∼100 μm) crystalline, shiny coating formed on the substrate and the wall of the quartz reactor. The quartz tube was removed and transferred to a drybox with the samples inside by closing the vacuum valves at both ends and detaching the tube from the vacuum/gas line. The coated silicon wafer substrate was mounted on XPS and ToF-SIMS sample holders under an argon atmosphere to prepare samples for the corresponding analyses. Controls for XPS analysis comprised a cleaned commercial silicon wafer (Silicon Quest International, silicon(100), boron-doped) and known standards: (a) single-crystal diamond, (b) diamond film, (c) glassy carbon, (d) pyrolytic graphite, (e) mineral graphite, and (f) HDLC (hydrogenated diamond-like carbon). The control for ToF-SIMS analysis comprised a cleaned commercial silicon wafer (Silicon Quest International, silicon(100), boron-doped). The coated substrate was also sent for Raman analysis (Charles Evans & Associates, Sunnyvale, CA), SEM characterization (S.S.W., University of Western Ontario, Canada, and Material Testing Laboratory, Pennington, NJ), and XRD analysis (IC Laboratories, Amawalk, NY).

ToF-SIMS Characterization. Cleaned commercial silicon wafers before and after plasma treatment to form a diamond film coating were characterized using a Physical Electronics TRIFT ToF-SIMS instrument. The primary ion source was a pulsed $^{69}Ga^+$ liquid metal source operated at 15 keV. The secondary ions were extracted by a ±3 keV (according to the mode) voltage. Three electrostatic analyzers (Triple-Focusing-Time-of-Flight) deflect them to compensate for the initial energy dispersion of ions of the same mass. The 400-pA dc current was pulsed at a 5-kHz repetition rate with a 7-ns pulse width. The analyzed area was 60 × 60 μm and the mass range was 0−1000 amu. The total ion dose was 7×10^{11} ions/cm^2, ensuring static conditions. Charge compensation was performed with a pulsed electron gun operated at 20-eV electron energy. To remove surface contaminants and expose a fresh surface for analysis, the samples were sputter-cleaned for 30 s using a 80 × 80 μm raster, with a 600-pA current, resulting in a total ion dose of 10^{15} ions/cm^2. Three different regions on each sample of 60 × 60 μm were selected using a microscope and analyzed. The positive and negative SIMS spectra were acquired. Representative postsputtering data are reported. The ToF-SIMS data were treated using "Cadence" software (Physical Electronics), which calculates the mass calibration from well-defined reference peaks.

XPS Characterization. A series of XPS analyses were made on the samples using a Scienta 300 XPS spectrometer at Lehigh University, Bethlehem, PA. The fixed analyzer transmission mode and the sweep acquisition mode were used. The aluminum X-ray incidence angle was 15°. The step energy in the survey scan was 0.5 eV, and the step energy in the high-resolution scan was 0.15 eV. In the survey scan, the time per step was 0.4 s, and the number of sweeps was 4. In the high-resolution scan, the time per step was 0.3 s, and the number of sweeps was 30. C 1s at 284.6 eV was used as the internal standard.

Raman Spectroscopy. Experimental and control samples were analyzed by Charles Evans & Associates, Sunnyvale, CA. Raman spectra were obtained with a LABRAM spectrometer (Dilor of Jobin Yvon) with a Spectrum One CCD (charge-coupled device) detector (Spex and Jobin Yvon) that was air- and Peltier-cooled. An Omnichrome HeNe laser (Melles Griot) with the light wavelength of 632.817 nm was used as the excitation source. The spectra were taken at ambient conditions and the samples were placed under a Raman microscope (Olympus BX40). Spectra of the film samples were acquired using the following conditions: the laser power at the sample was 4−8 mW, the slit width of the monochromator was 100 μm, which corresponds to a resolution of 3 cm^{-1}, the detector exposure time was 20 min, and 3 scans were averaged.

Experimental and control samples were also analyzed by Jobin Yvon Inc., Edison, NJ. Raman spectra were obtained with a LabRam HR system (Jobin Yvon Inc.) with a built-in microscope. The spectrometer had two interchangeable gratings with 1800 lines/mm, blazed at 500 nm, and was equipped with a liquid-nitrogen-cooled CCD detector (1024 × 256, BI, UV-coated). A helium−cadmium laser with the light wavelength of 325 nm was used as the excitation source. The spectra were taken at ambient conditions, and the samples were mounted under a Raman microscope. Spectra of the film samples were acquired at 3-s integration using the following conditions: the laser power at the sample was 15 mW and the slit width of the monochromator was 500 μm, which corresponds to a resolution of 2.5 cm^{-1}.

SEM Microstructure Analysis. The surface microstructure of the films was determined using a Hitachi-S-4500 field emission SEM at S.S.W., University of Western Ontario, Canada, and an Amray 1000 A SEM at Material Testing Laboratory, Pennington, NJ.

Characterization by X-ray Diffraction (XRD). The XRD patterns were obtained by IC Laboratories (Amawalk, NY) using a Phillips 547 diffractometer tuned for Cu Kα (1.540590 Å) radiation generated at 45 kV and 35 mA. The sample was scanned from 10−100° 2θ with a step size of 0.02° and 1 s/step.

Visible Spectroscopy and Balmer Line-Broadening Measurements. The widths of the 656.3-nm Balmer α line, 486.1-nm Balmer β line, 434.0-nm Balmer γ line, and 410.2-nm Balmer δ line emitted from hydrogen alone, xenon−hydrogen mixture (90/10%), helium−hydrogen mixture (90/10%), hydrogen−methane mixture (10−50/90−50%), and helium−hydrogen−methane mixture (48.2/48.2/3.6%) microwave discharge plasmas maintained in the microwave discharge cell shown in Figure 1 were measured with a high-resolution visible spectrometer capable of a resolution of ±0.006 nm according to methods given previously.[10,11] The spectra were recorded over the regions (410.05−410.35, 433.85−434.35, 485.90−486.40, and 656.0−657.0 nm). The total flow rate was controlled at 62.25 sccm using one mass flow controller for hydrogen alone and two in the case of a mixture of two gases. In the case of the helium−hydrogen−methane mixture, the methane flow at one mass flow controller was 2.25 sccm and the helium−hydrogen flow of 60 sccm was controlled by a second mass flow controller from a 50/50% mixture. The total pressure was 3 Torr, and the input power to the plasma was set at 40 W. The 667.816-nm He I line width was also recorded with the high-resolution (±0.006 nm) visible spectrometer on helium−hydrogen (90/10%) and helium microwave discharge plasmas. The visible spectrum was also recorded on the helium−hydrogen−methane mixture (48.2/48.2/3.6%) microwave discharge plasma.

To measure the absolute intensity, the high-resolution visible spectrometer and detection system were calibrated[12] with 5460.8-, 5769.6-, and 6965.4-Å light from a Hg−Ar lamp (Ocean Optics, model HG-1) that was calibrated with a NIST-certified silicon photodiode. The population density of the $n = 3$ hydrogen excited state N_3 was determined from the absolute intensity of the Balmer α (6562.8 Å) line measured using the calibrated spectrometer. The spectrometer response was determined to be approximately flat in the 4000−7000-Å region by ion etching and with a tungsten intensity calibrated lamp.

The electron density was determined using a Langmuir probe according to the method given previously.[13]

III. Results

ToF-SIMS. The positive ion ToF-SIMS spectra of a cleaned commercial silicon wafer before and after being

(10) Mills, R. L.; Ray, P. *New J. Phys.* **2002**, *4*, 22.1, available at www.njp.org.
(11) Mills, R. L.; Ray, P.; Dhandapani, B.; He, J. *J. Appl. Phys.* **2003**, *92*, 7008.
(12) Tadic, J.; Juranic, I.; Moortgat, G. K. *J. Photochem. Photobiol. A* **2000**, *143*, 169.
(13) Chen, F. F. Electric Probes. In *Plasma Diagnostic Techniques*; Huddleston, R. H., Leonard, S. L., Eds.; Academic Press: New York, 1965.

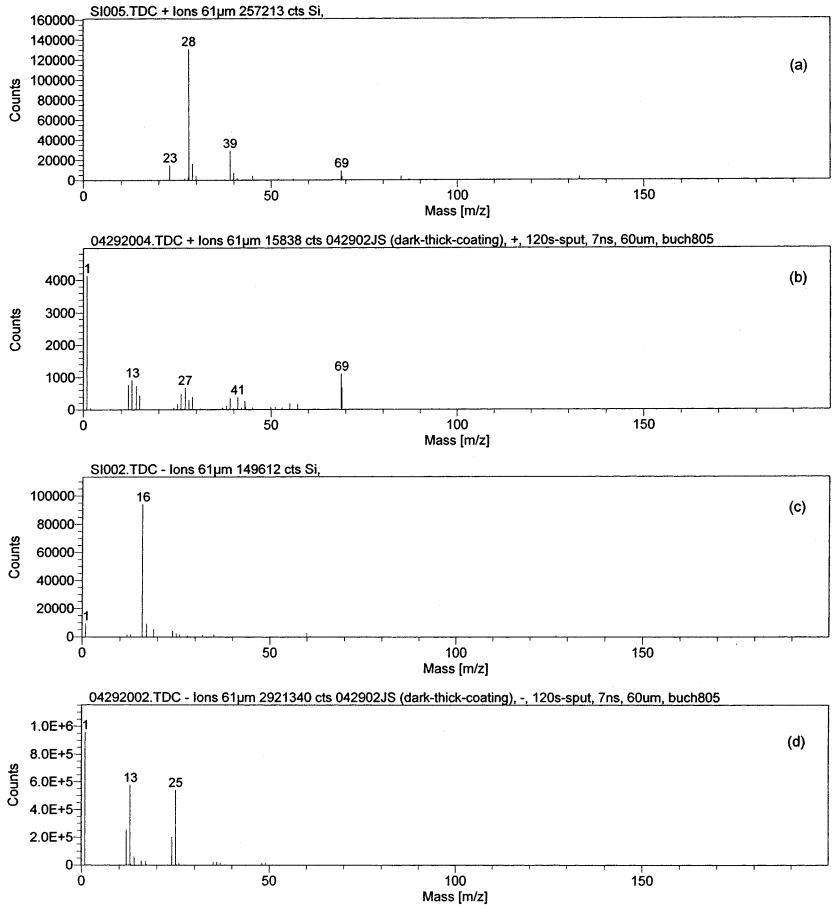

Figure 2. ToF-SIMS characterization of the substrate and carbon film. (a) The positive ion ToF-SIMS spectra ($m/e = 0-200$) of a noncoated cleaned commercial silicon wafer. (b) The positive ion ToF-SIMS spectra ($m/e = 0-200$) of a cleaned commercial silicon wafer coated by reaction of a helium−hydrogen plasma with CH_4 as the source of C that showed a large H^+ peak and trace hydrocarbon fragments $C_xH_y^+$. (c) The negative ion ToF-SIMS spectrum ($m/e = 0-200$) of a noncoated cleaned commercial silicon wafer. (d) The negative ion ToF-SIMS spectrum ($m/e = 0-200$) of a cleaned commercial silicon wafer coated by reaction of a helium−hydrogen plasma with CH_4 as the source of C that was dominated by hydride ion (H^-) and carbon ion (C^-). Very little oxide (O^-) or hydroxide (OH^-) was observed. An exceptional feature was the multimeric carbon clusters C_x^- at $m/e = 12, 24, 36, 48, 60, 72, 84, 96, 108, 120$.

coated with a carbon film are shown in parts (a) and (b), respectively, of Figure 2. The positive ion spectrum of the control was dominated by Si^+, oxides $Si_xO_y^+$, and hydroxides $Si_x(OH)_y^+$, whereas that of the carbon film sample contained no silicon-containing fragments. Rather, a large H^+ peak and trace hydrocarbon fragments $C_xH_y^+$ were observed. The $m/e = 69$ peak was due to the Ga^+.

The negative ion ToF-SIMS spectra of a cleaned commercial silicon wafer before and after being coated with a carbon film are shown in parts (c) and (d), respectively, of Figure 2. The control spectrum was dominated by oxide (O^-) and hydroxide (OH^-), whereas the spectrum of the carbon film was dominated by hydride ion (H^-) and carbon ion (C^-). Very little oxide (O^-) or hydroxide (OH^-) was observed. An exceptional feature was the multimeric carbon clusters C_x^- at $m/e = 12, 24, 36, 48, 60, 72, 84, 96, 108, 120$.

XPS. A survey spectrum was obtained over the region $E_b = 0-1200$ eV. The primary element peaks allowed for the determination of all of the elements present. The XPS survey scan of a cleaned commercial silicon wafer before and after being coated with a carbon film are shown in parts (a) and (b), respectively, of Figure 3. The major peaks identified in the XPS spectrum of the

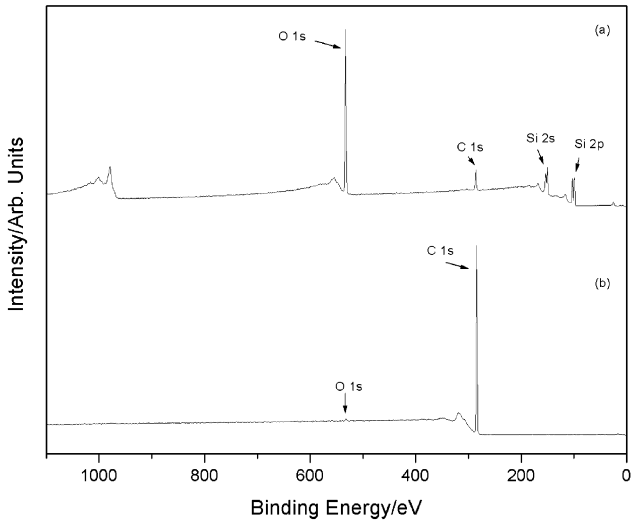

Figure 3. XPS characterization of the substrate and carbon film. (a) The XPS survey scan of a cleaned commercial silicon wafer. Only silicon, oxygen, and trace carbon contamination were observed. (b) The XPS survey scan of a cleaned commercial silicon wafer coated by reaction of a helium−hydrogen plasma with CH_4 as the source of C. Only carbon and trace silicon and oxygen contamination were observed.

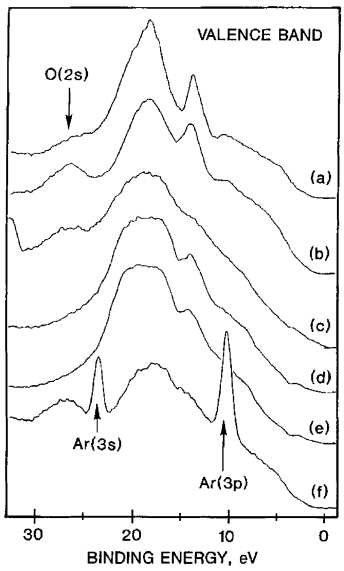

Figure 4. High-resolution XPS spectra (0−35 eV) of the valence band region of (a) single-crystal diamond, (b) diamond film, (c) glassy carbon, (d) pyrolytic graphite, (e) mineral graphite, and (f) HDLC.

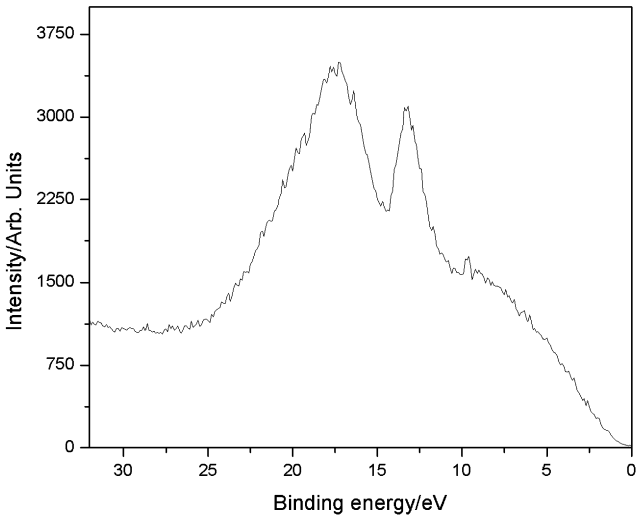

Figure 5. High-resolution XPS spectra (0−35 eV) of the valence band region of a cleaned commercial silicon wafer coated by reaction of a helium−hydrogen plasma with CH_4 as the source of C that showed features that matched single-crystal diamond.

control sample were O 1s at 533.0 eV, trace C 1s at 284.6 eV, and dominant Si 2s at 152.4 eV and Si $2p_{3/2}$ at 101.9 eV, whereas the carbon film sample comprised only carbon and trace silicon and oxygen contamination as indicated by the trace O 1s peak at 532.9 eV, the trace Si 2s at 153.2 eV and Si $2p_{3/2}$ at 102.2 eV, and the dominant C 1s peak at 284.6 eV.

The high-resolution XPS spectra (0−35 eV) of the valence band region of (a) single-crystal diamond, (b) diamond film, (c) glassy carbon, (d) pyrolytic graphite, (e) mineral graphite, and (f) HDLC are shown in Figure 4.[14] The corresponding XPS spectrum of the carbon film sample is shown in Figure 5. The film had a sharp peak at 13.2 eV and a broad peak at 17.4 eV, which matched

(14) Provided by A. Miller, Zettlemoyer Center for Surface Studies, Sinclair Laboratory, Lehigh University, Bethlehem, PA.

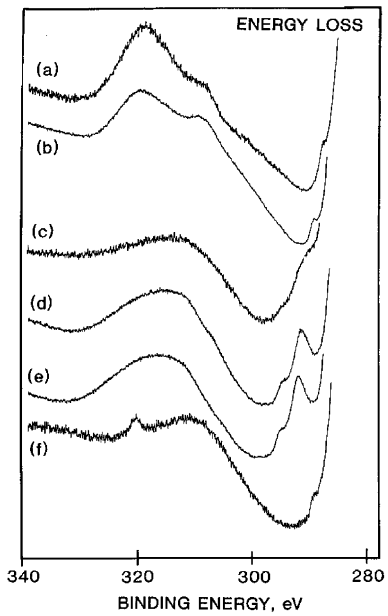

Figure 6. High-resolution XPS spectra (280−340 eV) of the C 1s energy loss region of (a) single-crystal diamond, (b) diamond film, (c) glassy carbon, (d) pyrolytic graphite, (e) mineral graphite, and (f) HDLC.

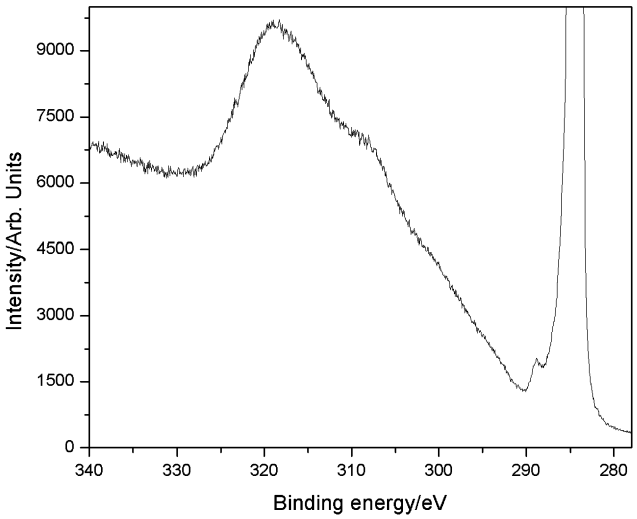

Figure 7. High-resolution XPS spectrum (280−340 eV) of the C 1s energy loss region of a cleaned commercial silicon wafer coated by reaction of a helium−hydrogen plasma with CH_4 as the source of C that showed features that matched single-crystal diamond.

the peak energies of single-crystal diamond rather than that of the other forms of carbon which were observed at higher binding energies. Also, no O 2s peak was observed in the region of 23 eV as shown in Figure 5.

The high-resolution XPS spectra (280−340 eV) of the C 1s energy loss region of (a) single-crystal diamond, (b) diamond film, (c) glassy carbon, (d) pyrolytic graphite, (e) mineral graphite, and (f) HDLC are shown in Figure 6.[14] The corresponding XPS spectrum of the carbon film sample is shown in Figure 7. Single-crystal diamond, diamond film, and HDLC have an energy loss feature that begins at about 290 eV, which is at a higher energy than that of the other possible forms of carbon as shown in Figure 6. The closest match to the shape of the energy loss feature of the carbon film is single-crystal diamond to which the film was assigned as a

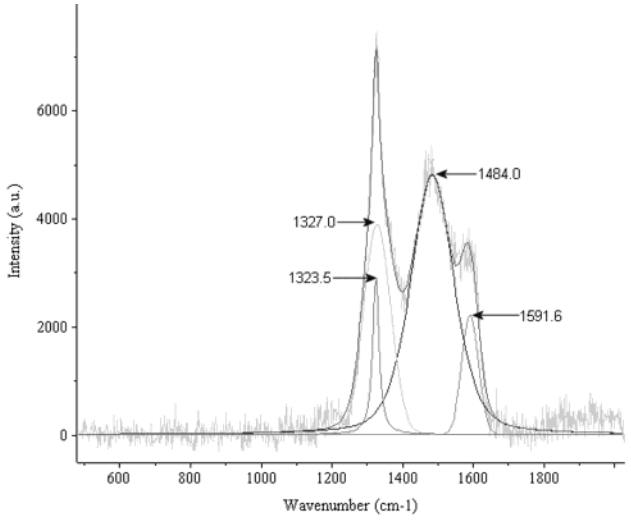

Figure 8. Raman spectrum recorded on the diamond film. The diamond band, D-band, G-band of DLC, and G-band of graphite were observed at 1323.5, 1327.0, 1484.0, and 1591.6 cm^{-1}, respectively. The 19.6-cm^{-1} fwhm of the diamond peak is characteristic of and identified the film as having polycrystalline diamond.

polycrystalline form based on the Raman and SEM characterizations given below.

Raman. The Raman spectrum of the corresponding region of the diamond film that was analyzed by ToF-SIMS and XPS is shown in Figure 8. Extensive curve fit analysis was performed. The peak positions, full-width-half-maximum (fwhm), and peak areas were calculated by the Gaussian curve fitting the baseline-corrected spectrum. The diamond band was observed at 1323.5 cm^{-1}, with a fwhm of 19.6 cm^{-1}, indicative of the polycrystalline nature of the diamond film.[15] In addition to the diamond band, the D-band, G-band of diamond-like carbon (DLC), and G-band of graphite were observed at 1327.0 cm^{-1} with a fwhm of 76 cm^{-1}, 1484.0 cm^{-1} with a fwhm of 130.2 cm^{-1}, and 1591.6 cm^{-1} with a fwhm of 46.5 cm^{-1}, respectively.

The ratio of the areas of the diamond peak to G-band of graphite, I_D/I_G, is considered an indirect measure of the carbon sp^3/sp^2 bonding ratio. The ratio I_D/I_G was 0.73. The Raman spectrum confirmed the XPS results that the film comprised diamond. On the basis of quantitative studies,[16,17] we estimate that the diamond composition of the films was well over 50%.

The Raman spectrum was repeatable as shown in Figure 9. A diamond band was observed at 1332 cm^{-1} for a second diamond film formed by helium−hydrogen−methane microwave discharge plasma (48.2/48.2/3.6%) CVD. In addition, the G-band of graphite was observed at 1580 cm^{-1}.

SEM Microstructure. Scanning electron microscopic images showed that the diamond films were polycrystalline. Individual 2−3-μm diameter clusters comprising 6−10 grains of diamond each having a grain size of 15−300 nm were observed as shown in Figure 10. In some areas of the surface, the clusters were embedded in an amorphous matrix. With increasing reaction time, the clusters increased in size, agglomerated, and then fused to form a thick uniform film as shown in Figure 11. The cross-sectional view of the film formed after 48 h showed a typical columnar growth pattern. The film thickness was in the range of 100−150 μm per 12−16 h of deposition time.

XRD. The X-ray diffraction (XRD) pattern of the diamond film for $2\theta = 40°-80°$ is shown in Figure 12. Since the beam size was larger than the film, the reflections were dominated by those from the silicon substrate. Diamond peaks were observed at $2\theta = 42.2°$ (rhombohedral (104)), 43.9° (cubic (111)), and 75.3° (cubic (220)).[18,19] The strongest diamond line showed very strong cubic (111) orientation. The peaks at 61.8°, 63.0°, and 76.2° are assigned to SiO_2/SiC, SiO_2, and Si, respectively. The broad peak at 69.4° belongs to the Si substrate plane and SiC, which is formed as a transition layer.[18−21]

Visible Spectrum and Line Broadening. The visible spectrum (275−700 nm) recorded on a helium−hydrogen−methane (48.2/48.2/3.6%) microwave discharge plasma is shown in Figure 13. The H α, β, γ, and δ lines observed at 656.3, 486.2, 434.1, and 410.2 nm, respectively, were significantly broadened as discussed infra. He I emission lines were observed at 667.8 and 468.57 nm. A progression of CH vibrational peaks were observed at 389 and 431 nm. The C_3 band was observed at 405.4 nm, and the C_2 Swan band ($A\ ^3\Pi_g \rightarrow X\ ^3\Pi_u$), $\Delta v = -1$, was observed at 468.2 nm. The H:C_2, CH:C_2, and CH:C_3 peak intensity ratios were similar to those reported by Elliott et al.,[3] which were correlated with the optimal conditions for diamond film quality and growth rate during diamond CVD using CH_4-CO_2 plasmas.

The Doppler-broadened line shape for atomic hydrogen has been studied on many sources such as a hollow cathode[22,23] and rf[24,25] discharges. The energetic hydrogen atom densities and energies were calculated[11] from the intensities and widths of the 656.3-nm Balmer α line emitted from microwave discharge plasmas of hydrogen compared with each of xenon−hydrogen (90/10%) and helium−hydrogen (90/10%) as shown in Figures14 and 15, respectively. The average helium−hydrogen Doppler half-width was not appreciably changed with pressure. The corresponding energy of 180−210 eV and the number density of 5×10^{14} ±20% atoms/cm^3, depending on the pressure, were significant compared to only 2−3 eV and 7×10^{13} ±20% atoms/cm^3 for pure hydrogen, even though 10 times more hydrogen was present. Xenon did not serve as a catalyst, and the plasma was much less energetic. Xenon−hydrogen showed no excessive broadening, correspond-

(15) Wagner, J.; Wild, Ch.; Koidl, P. *Appl. Phys. Lett.* **1991**, *59*, 779.
(16) Leeds, S. M.; Davis, T. J.; May, P. W.; Pickard, C. D. O.; Ashfold, M. N. R. *Diamond Relat. Mater.* **1998**, *7*, 233.
(17) Gilkes, K. W. R.; Prawer, S.; Nugent, K. W.; Robertson, J.; Sands, H. S.; Lifshitz, Y.; Shi, X. *J. Appl. Phys.* **2000**, *87*, 7283.
(18) Ownby, P. D.; Yang, X.; Liu, J. *J. Am. Ceram. Soc.* **1992**, *75*, 1876.
(19) Thewlis, J.; Davey, A. R. *Philos. Mag., B* **1956**, *1*, 409.
(20) Wang, Y. X.; Wen, J.; Guo, Z.; Tang, Y. Q.; Tang, H. G.; Wu, J. X. *Thin Solid Films* **1999**, *338*, 93.
(21) Kitabatake, M.; Deguchi, M.; Hirao, T. *J. Appl. Phys.* **1993**, *74*, 4438.
(22) Videnovic, I. R.; Konjevic, N.; Kuraica, M. M. *Spectrochim. Acta, B* **1996**, *51*, 1707.
(23) Alexiou, S.; Leboucher-Dalimier, E. *Phys. Rev. E* **1999**, *60*, 3436.
(24) Djurovic, S.; Roberts, J. R. *J. Appl. Phys.* **1993**, *74*, 6558.
(25) Radovanov, S. B.; Dzierzega, K.; Roberts, J. R.; Olthoff, J. K. *Appl. Phys. Lett.* **1995**, *66*, 2637.

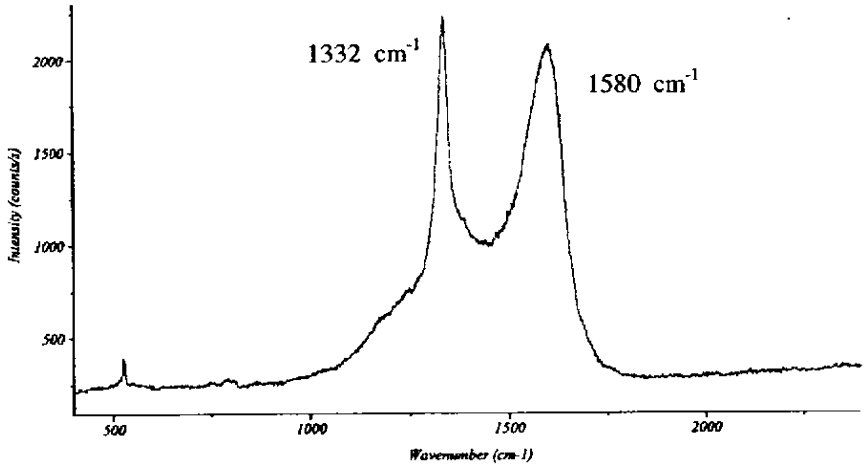

Figure 9. Raman spectrum of a second diamond film formed by helium−hydrogen−methane (48.2/48.2/3.6%) microwave discharge plasma CVD. A diamond band was observed at 1332 cm^{-1}. In addition, the G-band of graphite was observed at 1580.

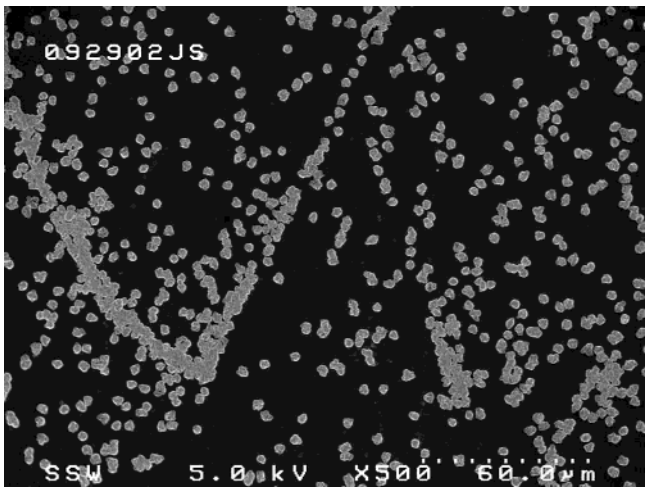

Figure 10. Surface SEM image at 500× that shows 2−3-μm diameter clusters comprising 6−10 grains of diamond, each having a grain size of 15−300 nm.

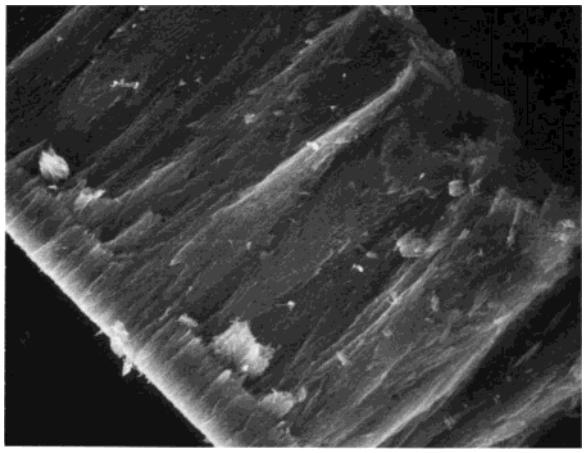

Figure 11. Cross-sectional SEM of the diamond film at 200× showing a typical columnar growth pattern. The film thickness was in the range of 500−600 μm after 48 h of deposition time.

ing to an average hydrogen atom temperature of 2−3 eV, and the atom density was also low, $3 \times 10^{13} \pm 20\%$ atoms/cm^3.

Significant broadening was also observed for the helium−hydrogen−methane (48.2/48.2/3.6%) plasma as shown in Figure 16. The average hydrogen atom temperature and density were high, 120−140 eV and $3 \times 10^{14} \pm 20\%$ atoms/cm^3, respectively, compared to 2−3 eV and $2 \times 10^{13} \pm 20\%$ atoms/cm^3 for a hydrogen−methane plasma. The percentage of hydrogen was varied from 10 to 50% with methane comprising the other compo-

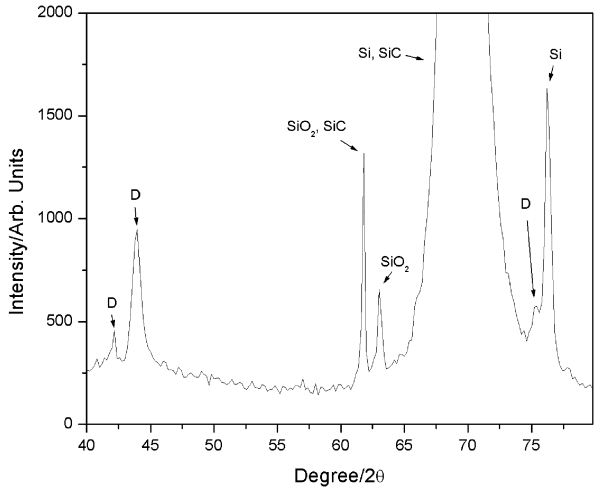

Figure 12. X-ray diffraction (XRD) pattern of a diamond film for $2\theta = 40°-80°$. The dominant peaks were due to silicon of the substrate. Diamond peaks were observed at $2\theta = 42.2°$ (rhombohedral (104)), 43.9° (cubic (111)), and 75.3° (cubic (220)).

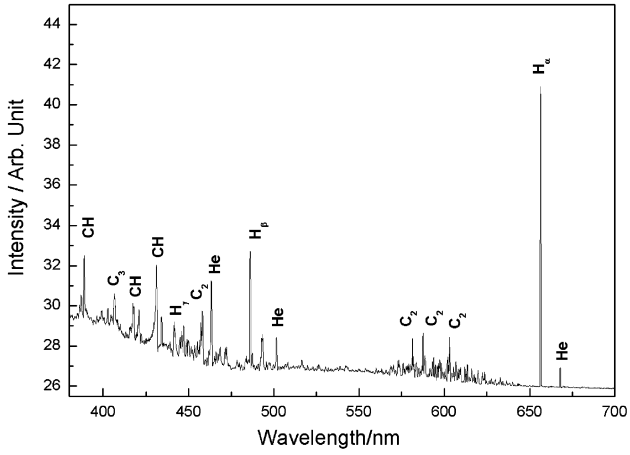

Figure 13. Visible spectrum (375−700 nm) recorded on a helium−hydrogen−methane microwave discharge plasma. CH, C_2, and C_3 emission were observed with significantly broadened H α, β, and γ lines.

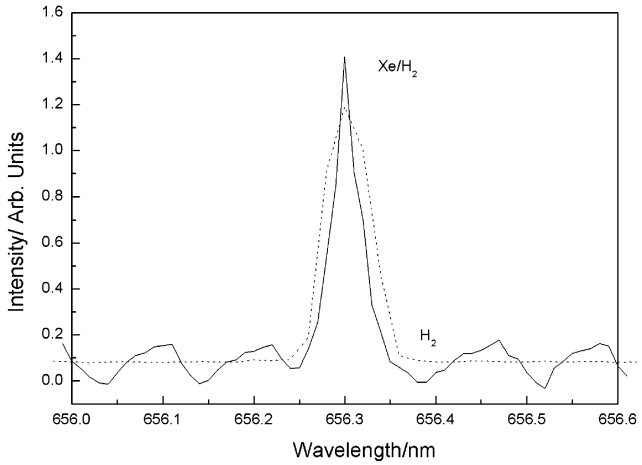

Figure 14. The 656.3-nm Balmer α line width recorded with a high-resolution (±0.006 nm) visible spectrometer on a xenon−hydrogen (90/10%) (solid curve) and a hydrogen microwave discharge plasma (dotted curve). No line excessive broadening was observed from either plasma, corresponding to an average hydrogen atom temperature of 2−3 eV.

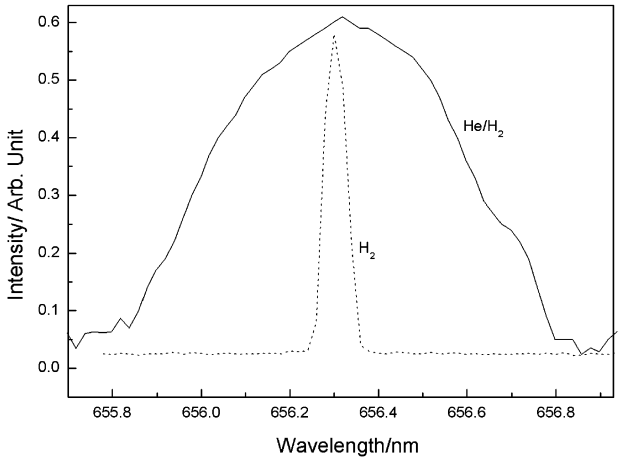

Figure 15. The 656.3-nm Balmer α line width recorded with a high-resolution (±0.006 nm) visible spectrometer on a helium−hydrogen (90/10%) and a hydrogen microwave discharge plasma. Significant broadening was observed for the helium−hydrogen plasma, corresponding to an average hydrogen atom temperature of 180−210 eV compared to 2−3 eV for a hydrogen plasma.

nent of the mixture. No broadening was observed with any of these plasmas.

Only the hydrogen lines were broadened. For example, the 667.816-nm He I line width was also recorded with the high-resolution (±0.006 nm) visible spectrometer on helium−hydrogen (90/10%) and helium microwave discharge plasmas. No broadening was observed in either case, whereas in each case, the broadening of the H β, γ, and δ lines were equivalent to that of the H α line.

We have assumed that Doppler broadening due to thermal motion was the dominant source to the extent that other sources may be neglected. This assumption was confirmed when each source was considered. In general, the experimental profile is a convolution of two Doppler profiles, an instrumental profile, the natural (lifetime) profile, Stark profiles, van der Waals profiles, a resonance profile, and fine structure. The electron density recorded with a Langmuir probe was 5 orders

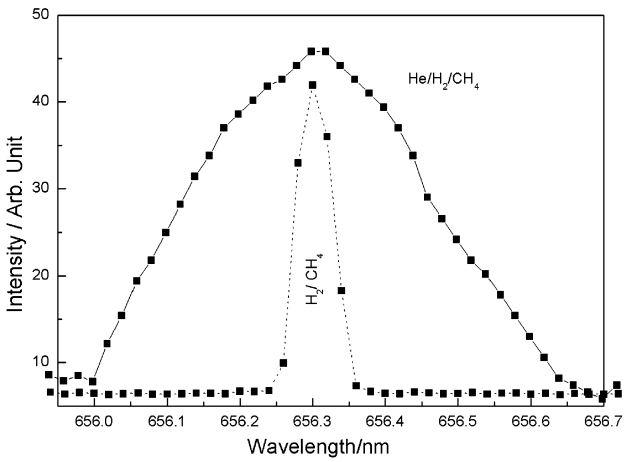

Figure 16. The 656.3-nm Balmer α line width recorded with a high-resolution (±0.006 nm) visible spectrometer on helium−hydrogen−methane (48.2/48.2/3.6%) and hydrogen−methane (10/90%) microwave discharge plasmas. Significant broadening was observed for the helium−hydrogen−methane plasma, corresponding to an average hydrogen atom temperature of 120−140 eV compared to 2−3 eV for a hydrogen−methane plasma.

of magnitude too low for detectable Stark broadening, and the contribution from each remaining source was determined to be below the limit of detection.[10,11]

IV. Discussion

In the previously developed CH_4-H_2 system and variations thereof, diamond formation occurs within a small domain about the CO tie line. Stringent conditions of a large excess of hydrogen, diamond seeding, and an elevated temperature are required. Similarly, in the CO_2-CH_4 system, diamond only formed within a range of a few percent from a 50/50% mixture. We observed for the first time that diamond was very reproducibly formed from a CH_4 carbon source with a helium−hydrogen plasma without the requirements of diamond seeding, an elevated temperature, high power, or an excess of hydrogen, or any particular former set of stringent conditions. Thus, a potential advancement in thin film diamond deposition has been shown.

The mechanism may be based on energetic hydrogen formed in the plasma reaction. Diamond and DLC are metastable materials; thus, continuous bombardment of the surface with energetic species that produce thermal and pressure spikes at the growth surface is required for deposition of diamond, DLC, and related films.[26] By quenching a beam of C^+ ions accelerated in an ultrahigh vacuum to a negatively biased substrate, Aisenberg and Chabot[27] were able to deposit DLC films for the first time. Rather than resulting in commercially useful processes, subsequently developed beam-type and sputtering production methods are essentially used for research. Exemplary methods discussed by Grill and Meyerson[28] are single low-energy beams of carbon ions, dual ion beams of carbon and argon, ion plating, rf

(26) Weissmantel, C. *Thin Films from Free Atoms and Molecules*; Klabunde, K. J., Ed.; Academic Press: New York, 1985; p 153.
(27) Aisenberg, S.; Chabot, R. *J. Appl. Phys.* **1971**, *42*, 2953.
(28) Grill, A.; Meyerson, B. *Synthetic Diamond: Emerging CVD Science and Technology*; Spear, K. E., Dismukes, J. P., Eds.; John Wiley & Sons: New York, 1994; p 91.

sputtering or ion-beam sputtering from carbon/graphite targets, vacuum-arc discharges, and laser ablation. With sputter deposition, amorphous DLC coatings can be prepared at low temperature due to high ion bombardment during the deposition of carbon. The absence of ion bombardment during carbon deposition leads to soft, conductive carbon films with no diamond-like properties. It has been shown that films with diamond-like properties are produced at ion energies of about 100 eV.[29,30]

V. Conclusion

Silicon substrates were coated by the reaction product of a low-pressure $He-H_2-CH_4$ (48.2/48.2/3.6%) microwave discharge plasma. The ToF-SIMS of the carbon film showed carbon clusters. The XPS of the valence band region and C 1s energy loss region, the Raman diamond peak at 1323.5 cm^{-1} with a fwhm of less than 20 cm^{-1}, and the SEM characterization showed that the film was a polycrystalline diamond with a high growth rate of about 10 μm/h. Diamond is proposed to form from CH_4 by the catalytic reaction of He^+ with atomic hydrogen, which forms an energetic plasma that was measured to have extraordinarily fast H.

Energetic species such as fast H formed in the helium−hydrogen microwave plasma, which showed extraordinary Balmer α line broadening corresponding to an average hydrogen atom temperature of 120−140 eV, may be the basis of the formation of the diamond film from CH_4. Without diamond seeding, production of polycrystalline diamond films on heterogeneous substrates was achieved under relatively low-temperature, low-power, mild conditions.

Acknowledgment. Thanks to A. Miller of Lehigh University for XPS analysis and very useful discussions and V. Pajcini of Charles Evans & Associates and O. Klueva of Jobin Yvon Inc. for Raman analysis and useful discussions.

CM020817M

(29) Ishikawa, J.; Ogawa, K.; Miyata, K.; Takagi, T. *Nucl. Instrum. Methods* **1987**, *B21*, 205.

(30) Rossi, F.; Andre, B. *Proceedings IP AT 1991*, Brussels; CEP Consultants: Edinburgh, UK, 1991; p 43.